# ENAS-BASED YOLOv8 IMPROVEMENT WITH JOINT STRUCTURE AND LOSS SEARCH FOR CORN SEEDLING AND WEED DETECTION
/
# 基于 ENAS 的 YOLOv8 改进方法：结合结构与损失函数搜索实现玉米幼苗与杂草检测

**Junnan HU [1], Hanyang WANG *[1], Yongcai MA [1], Dan LIU [2]**
[1] College of Engineering, Heilongjiang Bayi Agricultural University, Daqing, Heilongjiang/ China
[2] College of Civil Engineering and Water Conservancy, Heilongjiang Bayi Agricultural University, Daqing, Heilongjiang/ China
*Tel: +8613005357555; E-mail: michaelyang198217@163.com*
*Corresponding author: Wang Hanyang*
*DOI: https://doi.org/10.35633/inmateh-79-21*

***Keywords:** Corn seedling-weed detection; Efficient neural architecture search; YOLOv8; Edge deployment; Virtual spraying signal; Precision weeding*

## ABSTRACT
*Corn seedling and weed detection during the 2–5-leaf stage is essential for precision weeding, but similar morphology, field background interference, and the accuracy-efficiency trade-off limit the practical use of lightweight detectors. To address these problems, this study proposes Corn-Weed-ENAS, an improved YOLOv8-based detection model with joint structure and loss-function search. A differentiated ENAS search space was constructed for the backbone, neck, detection head, and loss function to automatically identify a compact architecture suitable for corn seedling-weed detection. A field image dataset of 2–5-leaf corn seedlings and weeds were collected in Heilongjiang Province, and comparative and ablation experiments were conducted against mainstream detectors. The proposed model achieved 97.3% mAP@0.5 with 2.5M parameters and 6.7 GFLOPs, showing a favorable balance between detection accuracy and lightweight deployment. To further verify its agricultural engineering applicability, an indoor simulated operation test was conducted on a Jetson Orin Nano Super platform using 20 pots of corn seedlings and weeds and a moving test vehicle at 1.2 m/s. In the virtual spraying signal verification, YOLOv8n produced five missed detections and one false detection, whereas Corn-Weed-ENAS produced three missed detections and no false detection. These results indicate that Corn-Weed-ENAS can provide more reliable weed localization and virtual trigger outputs for selective spraying decision support.*

## 摘要
*玉米 2~5 叶期苗草识别是精准除草的重要基础，但玉米幼苗与杂草形态相近、田间背景干扰复杂，且轻量化检测模型常存在精度与效率难以兼顾的问题。针对上述问题，本文提出一种结合结构搜索与损失函数搜索的 YOLOv8 改进模型 Corn-Weed-ENAS。该方法面向骨干网络、颈部网络、检测头和损失函数构建差异化 ENAS 搜索空间，自动获得适用于玉米苗草检测任务的紧凑型网络结构。本文采集黑龙江省 2~5 叶期玉米幼苗与杂草图像数据集，并与主流目标检测模型开展对比和消融试验。结果表明，所提出模型在 2.5M 参数量和 6.7 GFLOPs 条件下取得 97.3% mAP@0.5，实现了检测精度与轻量化部署之间的较好平衡。为进一步验证其农业工程应用适应性，本文基于 Jetson Orin Nano Super 平台开展了室内模拟作业试验，采用 20 盆玉米苗与杂草盆栽以及 1.2 m/s 移动试验车进行虚拟喷药信号验证。结果显示，YOLOv8n 出现 5 次漏检和 1 次误检，而 Corn-Weed-ENAS 仅出现 3 次漏检且无误检。结果说明，Corn-Weed-ENAS 能够为选择性喷药决策支持提供更可靠的杂草定位与虚拟触发输出。*

## INTRODUCTION
Weeds compete with crops for water, nutrients, and sunlight, suppressing crop growth and reducing yield and quality (*Hamuda et al., 2016; Islam et al., 2021*). Effective weed control during critical growth stages is thus essential for agricultural productivity (*Knezevic and Datta, 2015; Ramesh et al., 2021*). Current weed management relies on manual, mechanical, biological, and chemical methods (*Bajwa et al., 2015; Christensen et al., 2009; Wang et al., 2013*), with chemical control dominating globally due to its efficiency (*Harker and O'Donovan, 2013; Wei et al., 2010*). The 2–5-leaf stage is a critical weeding window for corn, where seedlings and weeds exhibit minimal morphological differences.

While targeted herbicide application can reduce weed damage, mechanical weeding is inefficient and labor-intensive, and chemical weeding causes pesticide waste and soil pollution, conflicting with green agriculture principles. Developing precise seedling-weed detection algorithms therefore holds significant academic and practical value for modernizing corn production and advancing sustainable agriculture (*Zhang, 2021*).

Driven by the growth of smart agriculture, machine vision and deep learning have become mainstream for agricultural target detection. The YOLO series of single-stage detectors is widely adopted for its balanced speed and accuracy (*Miao et al., 2025; Tang et al., 2025*). Among these, YOLOv8, with superior feature extraction, inference efficiency, and edge-deployment suitability, has been applied to corn seedling and weed detection (*Chu et al., 2025; Wang et al., 2026*). However, standard YOLOv8 faces notable limitations in real agricultural scenarios, including lighting variations, soil interference, seedling-weed occlusion, and morphological similarity at the 2–5-leaf stage. Existing studies have improved accuracy and lightweighting via complex dataset collection and module optimization, laying a foundation for seedling-stage weed detection (*Liu et al., 2022; Wang et al., 2026; Zhao et al., 2026*).

Recent studies have explored deep-learning-based crop and weed detection under natural field conditions. For example, MSRCR-YOLOv4-tiny was used to improve field corn weed detection under complex illumination, while improved YOLO-based models have been developed for corn-field weed detection and target spraying system design. These studies demonstrate the feasibility of lightweight object detection for agricultural weed control. However, most existing methods mainly focus on image-level detection accuracy and module-level network improvement. The connection between detection outputs and agricultural machinery decision signals, such as weed target-point localization and selective spraying triggering, is still insufficiently discussed.

Most current improvements rely on manually adding attention mechanisms and optimizing feature fusion modules, which depend heavily on researcher experience and consume substantial computational resources and time (*Ghosh et al., 2025; Jin et al., 2023; Yang et al., 2021*). Neural Architecture Search (NAS) addresses the limitations of manual network design; in particular, Efficient Neural Architecture Search (ENAS) drastically reduces search time and cost via parameter sharing, enabling automatic discovery of task-specific lightweight, high-performance networks, and has been widely used in computer vision (*Pham et al., 2018*). Currently, ENAS applications in object detection are limited to single-module local optimization, with scarce research in agriculture.

To meet the precision weed control needs of intelligent agricultural machinery, this study constructs a seedling-weed dataset for realistic corn seedling scenarios, focusing on 2–5-leaf corn and common weeds. A full-module ENAS-based joint optimization strategy is implemented for the YOLOv8 network, including fine-grained search of the backbone, neck, detection head, and loss function. Compared with manual module design, the proposed search strategy aims to obtain a compact architecture with better task adaptability. In addition to offline comparative and ablation experiments, this study further conducts an indoor simulated deployment experiment on a Jetson Orin Nano Super platform. The detection outputs are converted into weed center points and software-level virtual spraying trigger signals, thereby evaluating the potential of the proposed model as a perception and decision-support module for selective spraying or intelligent weeding equipment.

## MATERIALS AND METHODS

### *Data collection*

Data for this study were collected in Longfeng Town, Longfeng District, Daqing City, Heilongjiang Province. The corn varieties planted were Xianyu 696 and Xianyu 335. The collection environment and growth conditions are shown in Fig 1. The corn was planted in single rows on ridges, with a row spacing of 65 cm. Sampling took place from May to June 2025, when the corn was in the 2–5-leaf stage. Images were captured using a D435i stereo depth camera positioned 40-70 cm above the ground, with the camera's downward angle set between 60°and 90°. The dataset includes various lighting conditions (sunny, cloudy, overcast, etc., as well as early morning, morning, noon, afternoon, evening), different weed growth stages and species (such as Chenopodium, Apium, and Kochia), as well as varying levels of occlusion and weed density to ensure the dataset's generalizability. The dataset exhibits sufficient diversity, aiming to ensure its robustness in real-world application scenarios (*Le et al., 2021; Yang et al. 2025*).

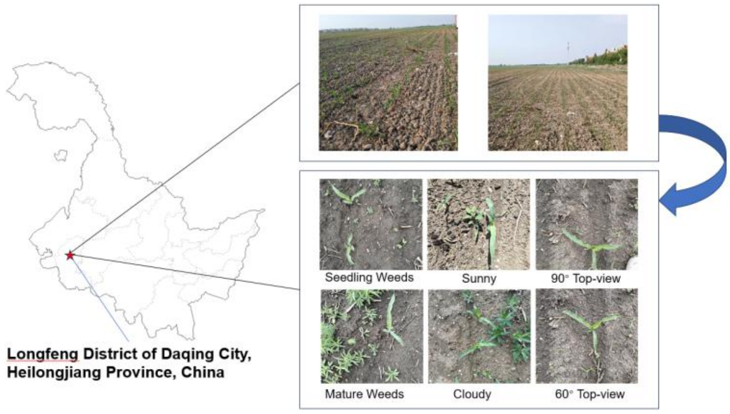


**Fig. 1 - Data collection environment and dataset details**

The data was manually screened to remove low-quality images with exposure issues (overexposure or underexposure) or blurriness, resulting in a total of 4,000 images, all saved in JPG format. During the preprocessing stage, a differentiated preprocessing strategy was employed to enhance the model's robustness in complex real-world scenarios. Specifically, while ensuring that the main content of the images remains recognizable, some images with slight blurring and uneven lighting were selectively retained with the aim of enabling the model to learn to perform recognition under suboptimal conditions. At the same time, all images were cropped to a uniform size to establish a standard input format. To further enhance the model's generalization ability and stability, this study implemented systematic data augmentation techniques to expand the training dataset by simulating a wider range of imaging variations. During the data augmentation phase, to enhance the model's robustness and generalization capabilities for corn seedling-weed detection recognition in complex field environments, a comprehensive augmentation strategy that included rotation, resizing, noise addition, and brightness adjustment was employed. The images were then annotated using the LabelImg tool and classified into two categories: corn and weeds. The dataset was randomly divided into training, validation, and test sets in an 8:1:1 ratio, ensuring that each set contained images from different environments (*Li et al., 2023*).

***Development of the ENAS framework***

This study builds upon the ENAS framework proposed by Pham et al. in 2018, retaining its core modules—the controller, hypernetwork, and reward signal—to construct a fine-grained search space covering all components of YOLOv8. An optimized ENAS network is proposed to achieve end-to-end automatic optimization of YOLOv8. Unlike traditional methods, this study focuses on the four key components of YOLOv8—the Backbone, Neck, Head, and loss function—to design differentiated, fine-grained search spaces and strategies that balance detection accuracy with model lightweighting, thereby improving search efficiency and convergence stability. The search process is as follows: the controller makes decisions regarding the architecture, the sub-architectures evaluate composite metrics on the hypernetwork validation set, and the controller updates the reinforcement learning policy based on these results, guiding the search toward a lightweight, high-performance solution. This framework integrates both global and local features required for identifying corn seedlings and weeds during the 2–5-leaf stage, striking a balance between accuracy and efficiency. The optimized, lightweight architecture selected is used for real-time, high-precision detection of corn seedlings and weeds in the field, achieving a Pareto optimal balance of accuracy, size, and speed.

***Corn-Weed-ENAS searchable object detection model architecture***

This study proposes the Corn-Weed-ENAS searchable object detection model, which centers on a weight-sharing supernetwork that integrates the ENASChoice module. It natively supports end-to-end architecture search and is tailored to meet the deployment requirements of agricultural embedded scenarios. The hypernetwork is designed according to the principle of layer-by-layer reconfigurability, which enables the construction of a fine-grained search space covering the entire network pipeline, including the core network components and supervisory signals. The search space consists of two main levels. First, fine-grained end-to-end search is performed across the Backbone, Neck, and Head. The backbone, neck, and detection head layers are encapsulated in ENASChoice modules, each integrating more than ten types of operation primitives, including standard convolutions, ghost convolutions, depthwise separable convolutions, attention mechanisms, and lightweight modules.

During the search process, the controller selects the optimal operation for each ENASChoice module, enabling end-to-end customization of the microarchitecture, from backbone feature extraction and multi-scale feature fusion to detection output. Second, flexible loss-function configuration is introduced. By incorporating multiple loss functions into the search space, the proposed method enables the joint optimization of the network architecture and the supervisory signal.

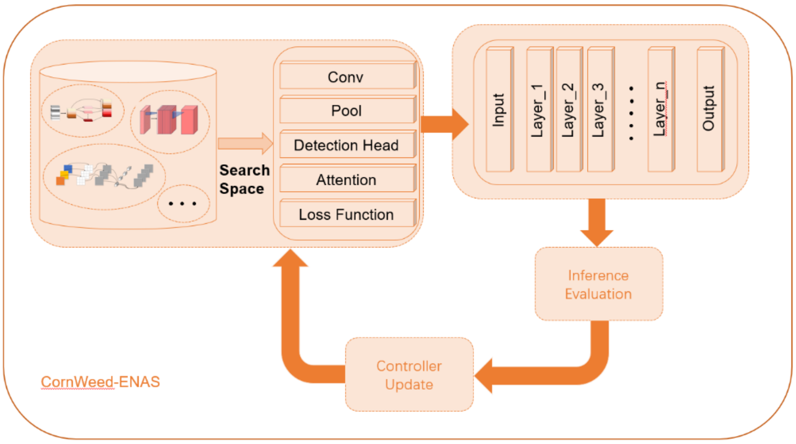


**Fig. 2 – Corn-weed-ENAS Workflow**

***Cooperative optimization algorithms and architecture mapping mechanisms***

Most traditional NAS algorithms are limited to optimizing the backbone network. To address this inherent limitation, this study proposes an improved Corn-Weed-ENAS co-optimization algorithm. Within the weight-sharing framework, the algorithm simultaneously performs joint optimization of architectural parameters and network weights, fully expanding the search space to encompass all critical dimensions that determine the model's final performance, covering the four core modules: Backbone, Neck, Head, and loss function. Throughout the architecture exploration process, the controller can dynamically balance multiple sets of interdependent key metrics. These metrics include model accuracy, computational complexity, and on-device inference speed. The ultimate goal of an algorithm is not the extreme optimization of a single metric. Its goal is to collaboratively identify the globally optimal architecture across multiple metrics, thereby achieving a paradigm shift from local component optimization to global system-level coordination. To achieve an efficient mapping from architectural decisions to an executable network topology, this study introduces a layer-by-layer mapping mechanism. The controller outputs a discrete selection index for each searchable unit. Using a prebuilt lookup dictionary, the system precisely maps indices to predefined operation keys or module instances, establishing a direct and stable link between high-level architectural decisions and low-level network implementation. Once the search is complete, the system instantiates a deterministic subnetwork from the hypernetwork based on the optimal selection sequence sampled by the controller. The subnet retains only the selected operations and modules. It also fully inherits the pre-trained weights from the hypernetwork, ultimately enabling a seamless transition from architecture search to a deployable model.

***Automatic search algorithms and implementation***

In the Corn-Weed-ENAS framework proposed in this study, the hyperparameters of the controller design and search process are set as follows. Architectural decisions are made using independent classification controllers, with each ENASChoice module and configurable component corresponding to a separate classification distribution. The maximum number of search rounds is set to 300. In each round, the controller samples a complete architectural configuration, corresponding to a specific subnet instance within the predefined full-stack search space. The key hyperparameters for policy-gradient updating include a baseline decay rate of 0.9 and an entropy regularization coefficient of 0.01.

After initializing the controller and the weight-sharing hypernetwork, the search iteration process is started. In each iteration, the current controller policy is evaluated as follows. First, the controller samples an architectural configuration, which is represented as a sequence of choice indices. Then, using a predefined lookup dictionary, this index sequence is mapped to specific operations and modules. Next, the selected subnet is activated in the hypernetwork, and 10% of the full dataset is selected for training to enable efficient subnet evaluation.

Finally, a reward value is calculated using a multi-objective function that balances detection accuracy and inference efficiency, thereby guiding the direction of the architecture search. The reward function is defined as follows:

$$R = R_{gating} + R_{main} + R_{bonus\_all} + R_{bonus\_pareto} \tag{1}$$

wherein: $R_{gating}$ is the gating penalty:

$$R_{gating} = -base_{penalty} - \alpha \times \max\left(0, map_{[0.5]min} - map_{[0.5]}\right) - \beta \times \max(0, map_{[0.5-0.95]min} - map_{[0.5-0.95]}) \tag{2}$$

where $base_{penalty} = 2.0$, $\alpha = 50.0$, $\beta = 30.0$, $map_{[0.5]min}$ and $map_{[0.5-0.95]min}$ are the minimum acceptable $map_{[0.5]}$ and $map_{[0.5-0.95]}$ values;

$R_{main} = \sum w_i \times gain_i + \sum w_j + save_j$ , where $gain_i$ denotes the relative improvement of metrics (precision, recall, $map_{[0.5]}$, $map_{[0.5-0.95]}$) over the baseline (normalized via tanh function with $s_{metric} = 0.01$ , and $save_j$ denotes the relative reduction of resources (parameters, FLOPs, weight size) compared to the baseline (normalized via tanh function with $s_{cost=0.05}$.

$R_{bonus\_all}$ is the "all-improve" bonus: a fixed value if the architecture outperforms the baseline in all metrics and underperforms in all resource indicators (zero if identical to the baseline);

$R_{bonus\_pareto}$ is the Pareto front bonus: scaled by the number of dominated architectures when the candidate is added to the Pareto front (Pareto tolerance tol= $1e-12$).

After receiving the reward, the algorithm executes the policy update step. The advantage function is computed as Advantage = Reward - Baseline, where Baseline refers to the exponential moving average of historical rewards. The controller's loss function is defined as follows:

$$L_{controller} = -log\pi_\theta(a) \cdot A - \lambda H(\pi_\theta) \tag{3}$$

Specifically, $\pi_\theta(a)$ denotes the joint probability that the IndependentCategoricalController samples the architectural configuration a under the current policy $\theta$ (product of independent categorical distribution probabilities for each configurable component). The negative logarithm of this probability, $-log\pi_\theta(a)$, corresponds to '-log_prob' in the code and serves as the core component of policy gradient computation. $A$ denotes the advantage function, computed as $A = R - B$; here, $R$ is the multi-objective reward calculated via Formula (1), and $B$ is the global exponential moving average baseline (independent of search state). This advantage value quantifies the relative quality of the current architectural configuration against the average performance. $H(\pi_\theta)$ represents the average entropy of the controller's categorical distributions (across all configurable components), weighted by the coefficient $\lambda$ to encourage architectural exploration.

The aforementioned iterative process proceeds cyclically until any of the following termination conditions is satisfied: (1) The preset maximum number of epochs is reached; (2) Algorithm performance converges, i.e., the improvement in the best fitness reward obtained over N consecutive generations falls below a preset threshold ε. Upon termination of the search, the architectural decision individual with the highest historical fitness is selected as the optimal solution. Subsequently, the system instantiates the corresponding operations and modules via the two-stage mapping process based on this optimal decision, directly extracts the corresponding weights from the pre-trained supernetwork, and assembles them into the final deployable lightweight detection model, thus completing the entire workflow from automated architecture search to efficient model derivation.

***Edge deployment and indoor simulated virtual spraying signal verification***

To further evaluate the practical applicability of the proposed Corn-Weed-ENAS model in agricultural machinery scenarios, an indoor simulated operation experiment was conducted using a Jetson Orin Nano Super development board. The development board was equipped with 8 GB memory and a 1024-core NVIDIA Ampere architecture GPU. A driver-free USB camera with a resolution of 0.3 megapixels was used as the image acquisition device. During the experiment, the camera center was installed 60 cm above the ground, and the optical axis of the camera was set at a downward angle of 60° relative to the horizontal plane. This configuration was used to simulate the visual perception condition of a small selective spraying or intelligent weeding platform.

Twenty pots of potted plants were arranged to construct the indoor simulated operation scene. Each pot contained 1–5 corn seedlings and weeds, forming different crop-weed distributions and partial occlusion conditions. During the experiment, the test vehicle moved along the horizontal line of the potted plants at a speed of 1.2 m/s.

The trained YOLOv8n and Corn-Weed-ENAS models were deployed on the Jetson Orin Nano Super platform for real-time detection. For each detected weed target, the center point of the bounding box was calculated and regarded as the potential spraying target point. A virtual spraying trigger signal was generated when the detected weed target satisfied the predefined trigger condition. Since no actual herbicide spraying device was connected in this experiment, the generated signal was used as a software-level virtual spraying signal to evaluate whether the model could provide usable perception outputs for subsequent selective spraying control.

This verification focused on the transformation from visual detection results to application-oriented decision signals. Missed detection was recorded when a weed target requiring a trigger signal was not detected by the model. False detection was recorded when a non-weed object or background region was incorrectly detected as a weed target and could lead to an unnecessary virtual spraying signal. The number of missed detections and false detections was compared between YOLOv8n and Corn-Weed-ENAS to evaluate the reliability of the proposed model in the simulated selective spraying scenario.

## RESULTS

### *Evaluation metrics and parameter settings*

To comprehensively and objectively evaluate the detection accuracy and target-recognition robustness of the detection models identified by the Corn-Weed-ENAS framework for corn seedling and weed detection, as well as their engineering deployment efficiency and lightweight characteristics when adapted to agricultural edge devices, this study combines conventional accuracy metrics from object detection with engineering-oriented deployment metrics to construct a multidimensional evaluation framework. The names, physical meanings, and descriptions of each evaluation metric are presented in Table 1. All subsequent calculations of these metrics follow the standard conventions used in the field of object detection.

**Table 1**

**Evaluation metrics**

| Index | Description |
|---|---|
| IoU=0.5 | The ratio of the intersection to the union between the model-predicted bounding box and the actual bounding box |
| AP | Average Accuracy at Different Recall Rates |
| mAP@0.5 | Mean Average Precision for corn seedling and weed detection at an IOU threshold of 0.5 |
| F1 score | Harmonic Mean of Precision and Recall |
| FPS | Number of images the model can process per second |
| Precision（P） | The ratio of accurately detected corn seedlings and weeds in the image to the total number of detected corn seedlings and weeds |
| Recall(R) | The proportion of correctly identified corn seedlings and weeds in the image relative to the total number of corn seedlings and weeds in the dataset |
| Weights | Weight Size(MB) |
| Parameters | Number of parameters in a model(M) |

Among these, IoU, AP, mAP@0.5, precision, recall and F1 score are accuracy metrics for quantifying the target localization and classification performance of corn seedling and weed detection models; FPS, model weight and parameter count are deployment metrics to evaluate inference speed and compactness, meeting the demands of agricultural edge computing applications. All tests were conducted on a Windows 11 system with an Intel Core i7-13700KF CPU and NVIDIA GeForce RTX 4070 Ti Super GPU, with PyCharm as the IDE and the core software stack: Python 3.10.19, PyTorch 2.7.1 and CUDA 12.6. For fair and comparable experimental results across all models, a unified set of hyperparameters was adopted: 640×640 input resolution, stochastic gradient descent (SGD) as the optimization algorithm, and 300 training epochs.

### *Comparative study*

Comparison models are categorized into three types covering object detectors of different generations and architectural paradigms: (1) YOLO baseline models (YOLOv5s, YOLOv7-tiny, and YOLOv8n, the search benchmark in this study); (2) the latest lightweight YOLO models (YOLOv11n, YOLOv12) representing state-of-the-art advances in lightweight visual recognition; (3) the classic two-stage detector Faster R-CNN, selected as the accuracy-oriented baseline. Detailed comparison results are presented in Fig. 3.

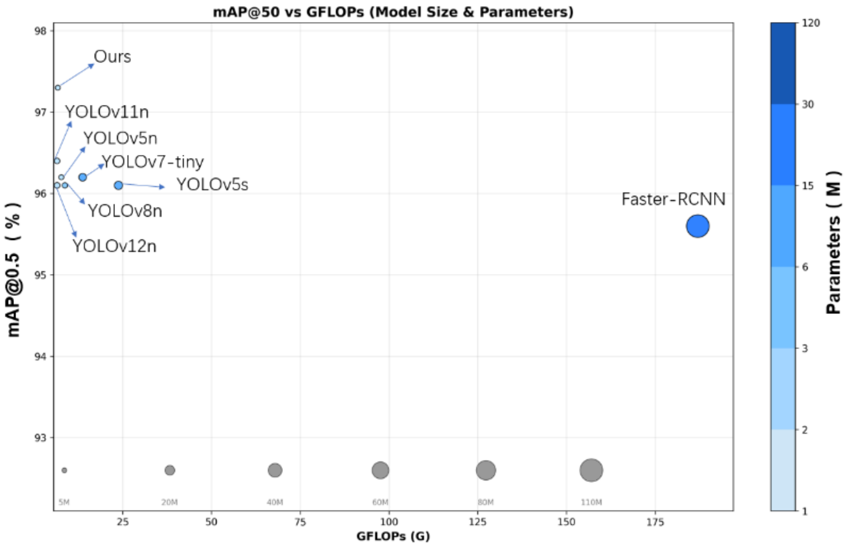


**Fig. 3 - Performance Comparison of Different Object Detectors on a Dataset of Corn Seedlings and Weeds**

**Table2**

**Other indicators not included in Fig 2**

| Indicator | YOLOv5s | YOLOv5n | YOLOv7 | YOLOv8n | YOLOV11n | YOLOV12n | Faster-RCNN | Ours |
|---|---|---|---|---|---|---|---|---|
| P | 93.9 | 93.6 | 93.7 | 92.7 | 93.6 | 93.6 | 77.9 | 94.6 |
| R | 92.1 | 93.0 | 93.3 | 93.2 | 92.6 | 93.2 | 96.1 | 96 |
| FPS | 66 | 204 | 119 | 180 | 241 | 240 | 8 | 234 |

The results show that the model identified by the Corn-Weed-ENAS framework achieved a 97.3% accuracy rate (mAP@0.5), with precision, recall, and F1 scores all outperforming the comparison algorithms, demonstrating the highest recognition accuracy. At the same time, with 5.2 million model weights, 2.5 million parameters, and only 6.7 billion FLOPs, it achieves improved performance while remaining lightweight.

***Results of edge deployment and virtual spraying signal verification***

The indoor simulated deployment experiment showed that both YOLOv8n and Corn-Weed-ENAS could be deployed on the Jetson Orin Nano Super platform and could output weed detection results and virtual spraying trigger signals under the moving operation condition. The test was conducted using 20 pots of potted corn seedlings and weeds. The camera was mounted 60 cm above the ground with a 60° downward viewing angle, and the test vehicle moved along the potted plants at a speed of 1.2 m/s.

Under the same deployment platform, camera configuration, operation speed, and virtual trigger strategy, YOLOv8n produced five missed detections and one false detection, whereas Corn-Weed-ENAS produced three missed detections and no false detection. Compared with YOLOv8n, Corn-Weed-ENAS reduced the number of missed detections by 40.0% and reduced the number of false detections from one to zero. This result indicates that the proposed Corn-Weed-ENAS model had more stable weed localization performance and lower risk of unnecessary virtual spraying signals in the simulated operation scenario.

Although this experiment did not involve actual herbicide spraying, it provided a software-level verification of the transformation from detection results to spraying decision signals. The results demonstrate that Corn-Weed-ENAS can not only achieve high detection accuracy in offline image evaluation, but also generate target-point outputs and virtual trigger signals on an edge device. Therefore, the proposed model has potential as a perception and decision-support module for selective spraying or intelligent weeding equipment.

**Table3**

**Edge deployment and virtual spraying signal verification results under the indoor simulated operation scenario**

| Model | Platform | Test scene | Missed detections | False detections | Relative change |
|---|---|---|---|---|---|
| YOLOv8n | Jetson Orin Nano Super | Indoor potted-plant simulated operation | 5 | 1 | Baseline |

| Model | Platform | Test scene | Missed detections | False detections | Relative change |
|---|---|---|---|---|---|
| Corn-Weed-ENAS | Jetson Orin Nano Super | Indoor potted-plant simulated operation | 3 | 0 | Missed detections reduced by 40.0%; false detections reduced to 0 |

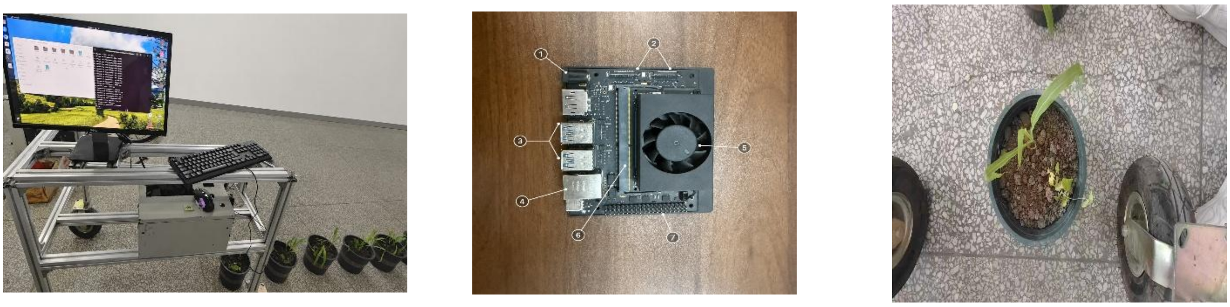

**Fig. 4 - Indoor simulated operation platform for edge deployment and virtual spraying signal verification.**
*(a) Overall indoor experimental platform with the test vehicle, deployment terminal, and potted samples;*
*(b) Jetson Orin Nano Super development board used for model deployment and real-time inference;*
*(c) Camera view of potted corn seedlings and weeds during vehicle movement.*

***Ablation experiment***

To validate the effectiveness of each structural module in the model and demonstrate the performance advantages of the Corn-Weed-ENAS model proposed in this paper, this section presents a systematic set of ablation experiments. The experiment uses the YOLOv8n model as the baseline and systematically decomposes it into four core search modules: the backbone network, the neck structure, the detection heads, and the loss function. It compares the detection accuracy and computational cost of the model under different combinations of these modules. Additionally, the experiment compares the final optimized model with the baseline model and the step-by-step search models to comprehensively evaluate the effectiveness of the model optimization. The evaluation metrics used in this experiment are the same as those in the comparative experiments. The experimental results are shown in Table 4.

**Table 4**

**Results of the ablation experiment**

| Model configuration | mAP@0.5 (%) | Precision (%) | Recall (%) | Weights (M) | Parameters (M) | FLOPs (G) |
|---|---|---|---|---|---|---|
| YOLOv8n (Baseline) | 96.1 | 92.7 | 93.2 | 6.3 | 3.0 | 8.1 |
| Only Backbone | 96.7 | 93.7 | 93.4 | 5.8 | 2.9 | 7.6 |
| Previous + Neck | 96.8 | 94.4 | 94.0 | 5.4 | 2.7 | 7.1 |
| Previous + Detection Head | 97.1 | 94.9 | 94.4 | 5.2 | 2.5 | 6.7 |
| Corn-Weed-ENAS | 97.3 | 95.1 | 94.6 | 5.2 | 2.5 | 6.7 |

Ablation experiments show that each module has a significant impact on model performance: Experiments show that the selection of the backbone, neck, head, and loss function all have a significant impact on model performance. The model offers notable advantages in terms of compactness, with 5.2 million weights, 2.5 million parameters, and 6.7 billion FLOPs. Its mAP@0.5 reached 97.3%, with the best performance across all accuracy metrics. It effectively addresses the challenge of balancing accuracy with lightweight design, outperforms both the baseline model and stepwise improvement models in overall performance, and offers significant practical value.

## CONCLUSIONS

Comparative and ablation experiments validated the effectiveness of the proposed Corn-Weed-ENAS model for corn seedling and weed detection. Compared with mainstream detectors including YOLO series models and Faster R-CNN, Corn-Weed-ENAS achieved 97.3% mAP@0.5 with 2.5M parameters and 6.7 GFLOPs, showing a favorable balance between detection accuracy, compactness, and deployment efficiency.

The ablation results further confirmed that the searched backbone, neck, detection head, and loss-function configuration jointly contributed to the final model performance.

To strengthen the agricultural engineering application of the study, an indoor simulated deployment experiment was conducted on a Jetson Orin Nano Super platform. Under a simulated moving operation condition with 20 pots of corn seedlings and weeds, YOLOv8n produced five missed detections and one false detection, whereas Corn-Weed-ENAS produced three missed detections and no false detection. The proposed model reduced missed detections by 40.0% and eliminated false detections compared with YOLOv8n. These results indicate that Corn-Weed-ENAS can provide more reliable weed localization and virtual spraying trigger outputs on an edge device.

Overall, Corn-Weed-ENAS can serve as a lightweight perception and decision-support module for selective spraying or intelligent weeding equipment. However, the deployment experiment in this study was a software-level virtual signal verification under an indoor simulated potted-plant scenario, and actual herbicide spraying and field weeding performance were not evaluated. Future work will connect the model with physical spraying or mechanical weeding actuators and conduct field-level operational tests to further verify its engineering applicability.

## ACKNOWLEDGEMENT

This study was financially supported by Accurate monitoring of soil crop information acquisition and real-time precision application technology and equipment research and development of medicine and fertilizer (No.: 2024ZXDXB45) Key Research and development Plan of Heilongjiang Province and Heilongjiangb Bayi Agricultural University Support Program from Daqing City, Grant No.ZRCPY202121.

## REFERENCES

[1] Bajwa, A. A., Mahajan, G., Chauhan, B. S. (2015). Nonconventional Weed Management Strategies for Modern Agriculture. *Weed Science*, Vol. 63(4), pp. 723-747, United States.

[2] Christensen, S., Søgaard, H. T., Kudsk, P., Nørremark, M., Lund, I., Nadimi, E. S., Jørgensen, R. (2009). Site-specific Weed Control Technologies. *Weed Research*, Vol. 49, pp. 233-241, United Kingdom.

[3] Chu, Y., Wei, Y. L., Liang, H. J., et al. (2025). Lightweight YOLOv8 Weed Detection Algorithm. *Journal of North China University (Natural Science Edition)*, Vol. 46, No. 4, pp. 489-498, Hebei/China.

[4] Ghosh, D., Ghosh, S., Jana, N. D., Biswas, S., Mallipeddi, R. (2025). Designing optimal Vision Transformer architecture using differential evolution for tomato leaf disease classification. *Computers and Electronics in Agriculture*, Vol. 238, pp. 110824, Netherlands.

[5] Hamuda, E., Glavin, M., Jones, E. (2016). A Survey of Image Processing Techniques for Plant Extraction and Segmentation in the Field. *Computers and Electronics in Agriculture*, Vol. 125, pp. 184-199, Netherlands.

[6] Harker, K. N., O'Donovan, J. T. (2013). Recent Weed Control, Weed Management, and Integrated Weed Management. *Weed Technology*, Vol. 27(1), pp. 1-11, United States.

[7] Islam, N., Rashid, M. M., Wibowo, S., Xu, C.-Y., Morshed, A., Wasimi, S. A., Moore, S., & Rahman, S. M. (2021). Early Weed Detection Using Image Processing and Machine Learning Techniques in an Australian Chilli Farm. *Agriculture*, Vol. 11(5), pp. 387, Netherlands.

[8] Jin, X., Xiong, J. H., Rao, Y., Zhang, T., Ba, W. J., Gu, S. F., Zhang, X. D., Lu, J. (2023). TranNas-NirCR: A method for improving the diagnosis of asymptomatic wheat scab with transfer learning and neural architecture search. *Computers and Electronics in Agriculture*, Vol. 213, pp. 108271, Netherlands.

[9] Knezevic, S. Z., Datta, A. (2015). The Critical Period for Weed Control: Revisiting Data Analysis. *Weed Science*, Vol. 63(SP1), pp. 188-202, United States.

[10] Le, V. N. T., Truong, G., & Alameh, K. (2021). Detecting Weeds from Crops Under Complex Field Environments Based on Faster RCNN. In: *IEEE 8th International Conference on Communications and Electronics (ICCE)*, pp. 350-355, Vietnam.

[11] Li, H. S., Shi, L., Fang, S., et al. (2023). Real-time Detection of Apple Leaf Diseases in Natural Scenes Based on YOLOv5. *Agriculture*, Vol. 13, No. 4, pp. 878, Switzerland.

[12] Liu, M. C., Gao, T. T., Ma, Z. X., et al. (2022). Field Weed Detection Model for Maize Based on MSRCR-YOLOv4-tiny. *Transactions of the Chinese Society for Agricultural Machinery*, Vol. 53, No. 2, pp. 246-255+335, Beijing/China.

[13] Miao, X., Wu, X., & Zhang, X. (2025). Lightweight corn leaf disease detection model based on YOLOV8N-LSCSBD. *INMATEH Agricultural Engineering*, Vol. 77, pp.373-382. DOI: https://doi.org/10.35633/inmateh-77-30. Romania.

[14] Pham, H., Guan, M. Y., Zoph, B., Le, Q. V., Dean, J. (2018). Efficient neural architecture search via parameter sharing. In: *Proceedings of the 35th International Conference on Machine Learning (ICML),* Vol. 80, Stockholm, Sweden.

[15] Ramesh, K., Kumar, S. V., Upadhyay, P. K., Chauhan, B. S. (2021). Revisiting the Concept of the Critical Period of Weed Control. *The Journal of Agricultural Science*, Vol. 159(9-10), pp. 636-642, United Kingdom.

[16] Tang, Y., Sun, J., Zhang, Y., Wang, C., Zhang, Z., & Shi, F. (2025). Kiwifruit flower detection using an optimized YOLOv11n architecture. *INMATEH Agricultural Engineering*, Vol. 77, No. 3, pp. 44-53, Romania.

[17] Wang, H. Z., Liu, H. T., Li, X. L., et al. (2025). Lightweight Lawn Heterogeneous Weed Detection Algorithm Based on Improved YOLOv8n. *Transactions of the CSAE*, Vol. 41, No. 10, pp. 157-165, Beijing/China.

[18] Wang, N., Shang, Z., Chen, K., et al. (2026). Weed Detection Method in Corn Field Based on Improved YOLOv5s. *Journal of China Agricultural University*, Vol. 31, No. 2, pp. 192-204, Beijing/China.

[19] Wang, P., Tang, Y., Luo, F., Wang, L., Li, C., Niu, Q., Li, H. (2022). Weed25: A Deep Learning Dataset for Weed Identification. *Frontiers in Plant Science*, Vol. 13, Switzerland.

[20] Wei, D., Chen, L., Ma, Z., Wang, G., & Zhang, R. (2010). Review of Non-chemical Weed Management for Green Agriculture. *International Journal of Agricultural and Biological Engineering*, Vol. 3(4), pp. 52-60, Beijing/China.

[21] Yang, X. J., Guo, M., Lyu, Q. S., Ma, M. (2021). Detection and classification of damaged wheat kernels based on progressive neural architecture search. *Biosystems Engineering*, Vol. 208, pp. 176-185, Netherlands.

[22] Yang, Z. J., Zhang, J. H., Liu, J. Q., et al. (2025). Lightweight Detection and Segmentation Method of Red Soil Aggregate Cracks Based on YOLOv8n-seg. *Transactions of the CSAE*, Vol. (Online), pp. 1-10, [2025-12-09], Beijing/China.

[23] Zhang, J. Y. (2021*). Design and Experiment of Intelligent Mechanical Weeding Device for Ridge Corn*. Harbin: Northeast Agricultural University, Heilongjiang/China.

[24] Zhao, J. G., An, M. L., Zhao, X. G., et al. (2026). Weed Detection Method and Target Spraying System Design of Corn Based on WEED-YOLOv10. *Transactions of the CSAE*, Vol. (Online), pp. 1-10, [2026-01-25], Beijing/China.